DOI 10.5162/Ultrasonic2025/A4-a1

Influence of Changes in Static Pressure on Sonoluminescence

Shuta Nakamura[1] and Ken Yamamoto[1]
[1]Department of Pure and Applied Physics, Kansai University Graduate School of Science and Engineering, 3-3-35 Yamate-cho, Suita-shi, Osaka, 564-8680, Japan
k610651@kansai-u.ac.jp

Abstract: Experimental observations and theoretical numerical calculations on the primary Bjerknes force were performed to determine the effect of static pressure changes on sonoluminescence (SL). The intensity of SL increased with increasing static pressure. The numerical calculations showed that under high static pressure, bubbles in standing waves are trapped at higher sound pressures. Bubbles trapped under higher sound pressure collapse more violently and the temperature inside the bubble increases.

Keywords: acoustic cavitation, sonoluminescence, static pressure, standing wave, primary Bjerknes force

1. Introduction

Ultrasonic cavitation is a phenomenon in which microscopic bubbles are generated by irradiation of ultrasonic waves into a liquid. Sonoluminescence (SL)[1] is known to depend on several parameters, including frequency, acoustic power, type of solute, type of dissolved gas, and liquid temperature. In this study, we focused on the parameter static pressure. Various experimental and theoretical studies have examined the effects of large static pressure changes (several MPa) on SL [2], but there are few studies on small changes in static pressure (several tens of kPa). Therefore, the purpose of this study was to clarify the effect of minute static pressure changes on SL and its associated factors.

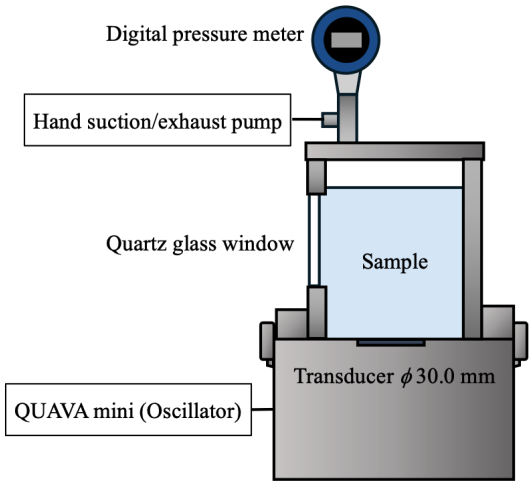

Fig. 1: Schematic diagram of the experimental system.

2. Materials and Methods

2.1. Experiment

Fig.1 shows a schematic diagram of the experimental system. A rectangular stainless steel sample chamber $(60 \times 60 \times 100\ mm)$ is attached to an ultrasonic generator (QUAVA mini, KAIJO Co., Ltd.) with a frequency of 430 kHz. A quartz glass window is installed in the side to allow measurement of SL. A digital pressure gauge (KDM30-α, Krone Corporation) and a hand suction exhaust pump are attached to the lid of the sample chamber to control the internal static pressure. Purified water was used as the test liquid, which was degassed by stirring under reduced pressure of 0.1 MPa for 1 h and then was stirred under an Ar atmosphere at ambient pressure for 1 h. The temperature of the samples was maintained at 13 ± 1°C by circulating cooling water outside the sample bath. Acoustic power was kept constant at 10 ± 1 W using the calorimetry method. SL spectra were measured with a spectrometer (SP2300i, Princeton Instruments) and CCD detector (Pixis100, Princeton Instruments). SL photographs were taken using a digital SLR camera (α7S, Sony Corporation) with an exposure time of 2 min.

2.2. Numerical calculation

Numerical calculations were performed for the vibration of a single bubble, neglecting interactions between bubbles. The bubble is assumed to always be spherical and its center is not displaced during one cycle. The bubble oscillations are described by the Keller-Miksis equation[3]:

DOI 10.5162/Ultrasonic2025/A4-a1

$$\left(1-\frac{\dot{R}}{c}\right)R\ddot{R}+\frac{3}{2}\dot{R}^2\left(1-\frac{1}{3}\frac{\dot{R}}{c}\right) = \left[1+\frac{\dot{R}}{c}+\frac{R}{c}\frac{d}{dt}\right]\frac{P_B}{\rho} \quad (1)$$

Here, R is the instantaneous bubble radius, t is time, an overdot denotes the time derivative, ρ is the density of the liquid, and c is the speed of sound in the liquid. The nonlinear term P_B can be expressed as

$$P_B=\left(P_0+\frac{2\sigma}{R_0}\right)\left(\frac{R_0}{R}\right)^{3\gamma}-\frac{2\sigma}{R}-\frac{4\mu}{R}\dot{R}-P_0+P_\infty \quad (2)$$

where R_0 is the initial radius of the bubble; σ and μ are the surface tension and viscosity in the liquid, respectively; P_0 is the static pressure; P_∞ is the external sound pressure; f is the ultrasonic frequency; and γ is the specific heat ratio of the gas in the bubble. The external sound pressure P_∞ assumes a standing wave and is represented by

$$P_\infty=-P_S\cos(kz)\sin(2\pi ft) \quad (3)$$

Here, k is the wavenumber, z is the position in the height direction, and $z=0$ is the position of the belly of the standing wave. The acoustic amplitude P_S was estimated from the acoustic power. Using the bubble radius R calculated by the Keller-Miksis equation, the primary Bjerknes force was calculated as follows[4]:

$$\vec{F_B}=-\langle\vec{F_p}\rangle=-\langle V\nabla p\rangle \quad (4)$$

Here, $\vec{F_p}$ is the instantaneous radiant force acting on the bubble and $\langle\ \rangle$ indicates the time average. The force $\vec{F_p}$ is given by

$$\vec{F_p}=\left(-\frac{4\pi}{3}\right)R^3kA\sin(kz)\sin(\omega t)\vec{e_z} \quad (5)$$

The change in bubble diameter was treated as an adiabatic process, and the maximum temperature inside the bubble was calculated using the following equation:

$$T_{max}=T_0\left(\frac{R_0}{R_{min}}\right)^{3(\gamma-1)} \quad (6)$$

here T_0 is the initial temperature inside the bubble The above equations were solved using MATLAB's ODE45s solver, with absolute and relative tolerances of 1×10^{-9}. The gas inside the bubble was assumed to be Ar. The initial conditions were as follows: $R(0)=R_0$, $\dot{R}(0)=0$, $T_0=286.15$ K, $f=430$ kHz, $\rho=1000\ \mathrm{kg/m^3}$, c=1482 m/s , σ=72.75×10^{-3} N/m, μ=1.002×10^{-3} Pa·s, γ=1.67,and P_w=10 W.

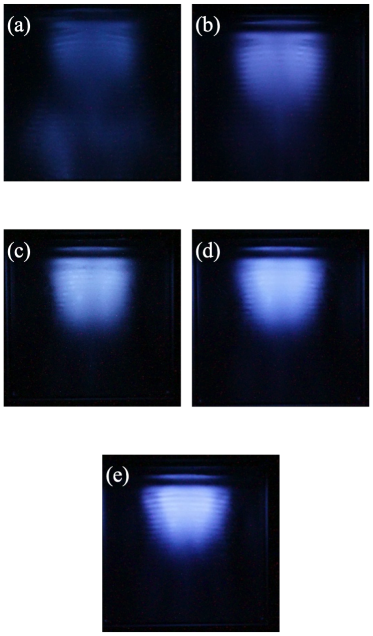

Fig. 2: Photographs of SL taken under different static pressures. All photographs were taken with an exposure time of 2 min.

3. Results and Discussion

3.1. SL Observations

Changes in SL intensity and emission distribution in response to variations in static pressure were observed. Fig. 2 show photographs of SL observed under different static pressures. As the static pressure was increased, stronger light emission was observed near the liquid surface. Conversely, as the static pressure was decreased, the emission distribution extended further toward the bottom of the sample chamber. Previous studies have also reported that light emission is concentrated near the liquid surface, which can be explained by the ratio of standing wave and traveling wave components [5]. A standing wave arises from the interference between a traveling wave and its reflected wave. In regions farther from the liquid surface, attenuation of the sound wave causes the reflected wave to become weaker than the traveling wave, hindering formation of a standing wave. As a result, the traveling wave component becomes dominant. In areas where the traveling wave component is strong, bubbles experience radiation force from the traveling wave and move toward the liquid surface. In such regions, bubble collapse events capable of generating SL are less likely to occur. On the other hand, near

DOI 10.5162/Ultrasonic2025/A4-a1

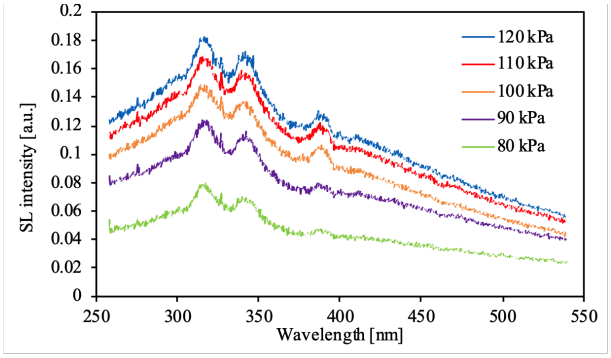

Fig. 3: SL spectra in Ar saturated water at different static pressures.

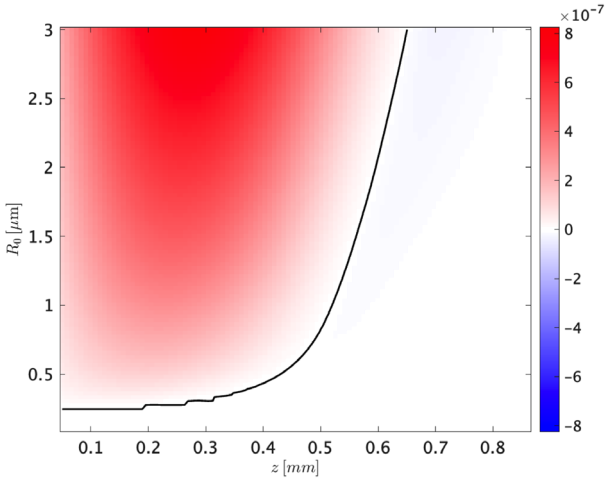

Fig. 4: Heat map showing the magnitude of the primary Bjerknes force for at position z and for initial bubble radius R_0. Static pressure is 100 kPa. The line indicates the point where $\vec{F}_B$=0.

the liquid surface, the attenuation of the traveling and reflected waves is roughly the same, leading to a stronger standing wave component. In regions with a strong standing wave component, bubbles are trapped within the standing wave due to the primary Bjerknes force [4] and oscillate in stable positions. As a result, SL is concentrated in these regions. Fig. 3 shows the measurement results of SL intensity. Based on the SL spectrum, the intensities of both the broadband component and the OH radical peak were calculated. As the static pressure was increased, the intensities of both the broadband emission and the OH radical peak increased accordingly.

3.2. Numerical Calculation of the Primary Bjerknes force

To examine the equilibrium positions of bubbles within a standing wave, a numerical calculation of the primary Bjerknes force was conducted. The time average over one acoustic cycle was taken, where a force pushing the bubble away from (resp. toward) the pressure antinode was taken as positive (resp. negative). Fig.4 shows a heat map representing the magnitude of the primary Bjerknes force as a function of position z and initial bubble radius R_0 under a static pressure of 100 kPa. When a bubble is located far from the pressure antinode, it experiences a negative radiation force pulling it toward the antinode. However, as it approaches the antinode, it eventually experiences a positive radiation force, pushing it away. As this occurs, the bubble continues to expand even into the second half of the acoustic cycle, making the contribution of the latter half dominant. As a result, the bubble becomes trapped at the position where the Bjerknes force is zero $\left(\vec{F}_B = 0\right)$. The trapping position depends on the initial bubble radius R_0, with smaller bubbles tending to be trapped closer to the pressure antinode.

Fig. 5 shows the dependence of the bubble trapping position on static pressure. Numerical calculations revealed that, for all initial bubble radii, the bubbles become trapped closer to the pressure antinode with increasing static pressure. This indicates that the bubbles are trapped in regions with higher acoustic pressure. The bubbles move closer to the antinode because the time required for the bubbles to collapse becomes shorter with increasing static pressure. As a result, the contribution from the latter half of the acoustic cycle becomes smaller, leading to trapping positions closer to the antinode.

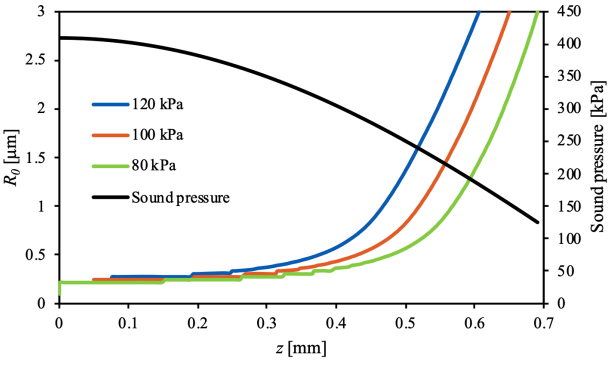

Fig. 5: Size of bubbles trapped at position z under different static pressures. The second vertical axis shows the sound pressure that the bubble at position z receives from the standing wave.

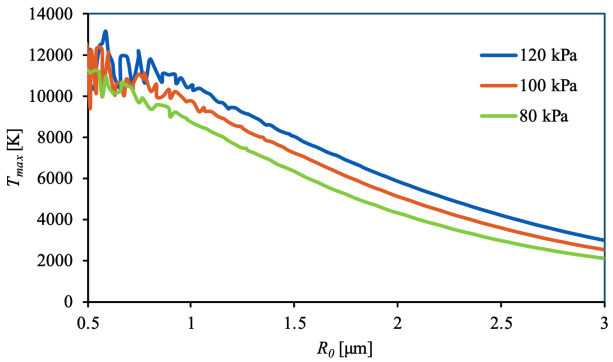

Fig. 6: Maximum temperature inside the bubble at the bubble trap position. z corresponding to R_0 was determined from Fig. 5.

Fig. 6 shows the maximum temperature inside the bubble at the trapping position. Based on the results from Fig. 5, the acoustic pressure corresponding to each initial bubble radius R_0 and static pressure P_0 was determined. The maximum temperature increased with rising static pressure. The reason for this was that the change in bubble position due to the increase in static pressure caused the bubble to experience higher acoustic pressure, resulting in more violent collapse. The internal bubble temperature is a crucial parameter in determining SL intensity, and its dependence on static pressure shows a trend similar to that observed in Fig.3. These results suggest that the equilibrium position of the bubble in the standing wave may be one of the key factors influencing SL intensity.

4. Conclusion

An increase in SL intensity and a change in the emission distribution were observed with increasing static pressure. Numerical calculations revealed that, with increasingstatic pressure increases, bubbles become trapped closer to the pressure antinode of the standing wave. Bubbles subjected to stronger acoustic pressure undergo more violent collapse and reach higher maximum temperatures. This study enhances our understanding of static pressure as a key parameter in ultrasonic cavitation and contributes to the determination of efficient operating conditions for industrial applications such as ultrasonic cleaning and sterilization.

References

[1] P.-K. Choi and *et al.* "Na emission and bubble instability in single-bubble sonoluminescence". In: *Ultrasonics Sonochemistry* 38 (2017), pp. 154–160. DOI: 10.1016/j.ultsonch.2017.03.015.

[2] S. Merouani and *et al.* "Review on the impacts of external pressure on sonochemistry". In: *Ultrasonics Sonochemistry* 106 (2024), p. 106893. DOI: 10.1016/j.ultsonch.2024.106893.

[3] J. B. Keller and *et al.* "Bubble oscillations of large amplitude". In: *Journal of the Acoustical Society of America* 68 (1980), pp. 628–633. DOI: 10.1121/1.384720.

[4] T. J. Matula and *et al.* "Bjerknes force and bubble levitation under single-bubble sonoluminescence conditions". In: *Journal of the Acoustical Society of America* 102 (1997), pp. 1522–1527. DOI: 10.1121/1.420065.

[5] J. Lee and *et al.* "Spatial Distribution Enhancement of Sonoluminescence Activity by Altering Sonication and Solution Conditions". In: *Journal of Physical Chemistry B* 112 (2008), pp. 15333–15341. DOI: 10.1021/jp8060224.